International Journal of Aviation Science and Technology

Research Article

The Detection Capability of Laser Fuze in Fog, Mist, and Haze Using Monte Carlo Simulations

Hoang Linh Nguyen[1],Trung Dung Pham[2],Chung Thanh Nguyen[3],Hong Son Tran[4]*

[1] *Faculty of Control Engineering, Le Quy Don Technical University, 100000 Hanoi, Vietnam*
nghoanglinh86@gmail.com - 0000-0002-2041-6383
[2] *Faculty of Control Engineering, Le Quy Don Technical University, 100000 Hanoi, Vietnam*
thchdung@gmail.com - 0000-0003-1812-3642
[3] *Faculty of Control Engineering, Le Quy Don Technical University, 100000 Hanoi, Vietnam*
nguyenthanhchung@lqdtu.edu.vn - 0000-0003-1182-8746
[4] *Faculty of Control Engineering, Le Quy Don Technical University, 100000 Hanoi, Vietnam*
tranhongson@lqdtu.edu.vn - 0000-0002-7956-2377

Abstract

When choosing a laser wavelength for proximity fuze with high accuracy requirements, the weather condition is a considerable element. Hence, the paper developed a laser detection model in different conditions based on the Monte Carlo method to evaluate the detection capability. As the atmospheric attenuation is a function of the wavelength, there is a conception that the laser pulsed fuze with 1550 nm light suffers from less atmospheric attenuation than 785 or 850 nm laser in all weather conditions (Pratt, 1969). However, in foggy weather (visibility <500 m), the results showed that laser attenuation appeared to be wavelength independent, i.e. the wavelengths of 785 nm, 850 nm, and 1550 nm are equally all attenuated equally by fog. Furthermore, the simulations also allowed the prediction of transmission, as well as the effects of energy scattering and absorption. This paper can provide guidance and reference for the application of laser wavelengths in the laser fuze.

Keywords

Atmospheric attenuation,
Laser pulse fuze,
Monte Carlo,
Detection capability

Time Scale of Article

Received 15 December 2022
Revised to 27 April 2023
Accepted 29 April 2023
Online date 28 June 2023

1. Introduction

A laser fuze is a weapon component using lasers to identify close-range targets, often at a distance of fewer than 20 meters, and regulates the time of ammunition explosion depending on the information from the identified targets (Hu et al., 2017). However, the near-infrared spectrum, which almost laser fuze output wavelengths presently utilize, is significantly influenced by the bad atmosphere (Liu, 2017). In contrast to radio wavelengths, optical wavelengths correspond to particles of the same size as vapor; consequently, atmospheric phenomena such as cloud, fog, and haze scatter laser beams (Kavehrad and Hamzed, 2005). The key optical phenomena which influence the detection performance of laser fuze in cloudy conditions are scattering, absorption and reflection. The absorption and scattering of the clouds reduce the energy of the signal reflected from the target in clouds, making it hard for the fuze to detect the target. The detection capabilities of the laser fuze are therefore assessed using parameters that take into account light propagation in cloudy environments. A simulation of the photon path through different weather conditions has been proposed from the three primary optical processes.

Fog, mist, and haze are visibility types in the cloud medium. A cloud is generated when water vapor from evaporation toward the sky and condenses at high altitudes. Clouds arise when vapor condenses around dust and smoke particles. Fog originally emerged when there is a lot of moisture in the air, wind, and a stable atmosphere. Haze, on the other hand, is a collection of aerosols that have been discharged into the air, such as

*: Corresponding Author Hong Son Tran, tranhongson@lqdtu.edu.vn
DOI: 10.23890/IJAST.vm04is01.0105

dust, smoke, or salt particles. Photon is absorbed and scattered by various aerosols and gaseous molecules in the atmosphere.

A current transmitter with a laser pulse electronics in proximity fuze use diode bars operating in the wavelength region from 780 to 860 nm. The wavelength and power may also be regulated by the safety class required. However, the most powerful semiconductor lasers can be found in the wavelength range of 800-900 nm. The semiconductors are GaAs, GaAlAs or InGaAs and operate over wavelength range of 850 to 910 nm. Lasers with a small output power (1 mW – 50 mW), small size, and long wavelength (1300 – 1550 nm) can be used in pulsed TOF laser fuze. These lasers use a Nd: YAG crystal as a lasing medium, and also operate in the near-infrared range, 1550 nm.

Concerning the echo signal in clouds, Wang et al. investigated the transmittance of near-, mid-, and far-infrared lasers in aerosols and discovered that the latter had higher transmittance than the former (Wang et al., 2013). The lasers used are typically in the near-infrared spectrum, as many mediums are relatively transparent at these wavelengths (Sato et al., 2002). Because of their efficiency and light weight, diode lasers are the most commonly used, though Nd:YAG and fiber lasers are also used (Kagan et al., 2002). Although they are created by the combined effects of the laser transmittance, scattering, and target reflection in clouds, target echoes in clouds are calculated just only on the transmittance. Winker and Poole simulated the cloud backscattering echo for near-infrared lidar in relation to this phenomenon (Winker and Poole, 1995). By using a near-infrared lidar, Chudamani et al. evaluated the backscattering cross-section of tropospheric aerosols (Chudamani et al., 1996). The backscattering coefficients of aerosols that resemble clouds were theoretically calculated by Srivastava et al. using near- and far-infrared lidars (Srivastana et al., 1992). Because the conclusions of these studies are all about long detection distances (generally a few hundred meters to several hundred kilometers), they are inapplicable for laser fuze with short detection ranges.

The echo energy in the presence of the target and transmission of the laser can be used as a parameter for evaluating the detection capability of laser fuze in visibility conditions. The echo energy is influenced by the attenuation coefficient. While the transmission of a laser beam is absorbed and dispersed by air molecules, suspended dust, and aerosols as it travels through the atmosphere. The purpose of the paper is to develop a model to evaluate the ability of a laser fuze to detect the target through a cloudy environment. A model based on Monte Carlo Ray Tracing (MCRT) is presented to study light passing through a scattered medium. A cloud medium is a scattering medium containing aerosols and particles, such as smoke, raindrops, etc. A photon will collide with the cloud particle when it propagates in clouds. For the photons that are returned and received successfully by the laser receiver, the energy and moment at which they are received are recorded. This direct simulation approach has the advantage of allowing for highly flexible computations, but this method needs a huge amount of computation. Because it is a statistical technique, it is necessary to calculate a large number of photons to reduce the variance in the results.

Although the model described here was designed to investigate a variety of optical effects on space-based photons, it is quite general and can be applied to a wide range of problems. The model can explain how scattering and absorption parameters (μ_{sca}, μ_{abs}) affect distance measurement. The model can estimate energy transmission and absorption, as well as a total reflection at the target surface, in order to construct a model for predicting light propagation through clouds and analyzing the detecting capabilities of the laser fuze. A successful model would allow its predictions to be used to assess the accuracy of measurements.

2. Methods

A detection model is built using the Mie scattering theory and the Monte Carlo method. In Figure 1, a coordinate system is established, with the laser emission window as the origin and the axial direction of the emitted laser as the z-axis. The technique uses a Monte-Carlo approach to generate photons through the atmospheric paths, counting for absorption, scattering and reflection from the target surface. The laser energy is represented by the number of photons. The atmospheric effects limit the capabilities of laser fuze since the laser pulse travels through the air, and some of the energy is absorbed and scattered by atmospheric molecules and suspended dust and aerosols.

2.1 Photon Positioning and Initial Conditions

In this paper, the term "photons" used in this simulation is not equivalent to photons found in particle physics, which represent a conceptual unit of light in the simulation. Each photon in the simulation is given a weight, denoted by w. Each photon began by pointing directly into the cloudy environment, where each photon began with a random, forward angle. Each photon moves along a random path length, absorbing a fraction of its weight along the way. The scattering direction is updated after each step randomly. When the laser transmitter emits photons, the initial energy of photons is $w = 1$. As the photon propagates through the atmospheric cloudy paths, it slowly loses weight at each scattering event. To prevent photons from continuing indefinitely, the photon is removed when its weight falls below a certain threshold.

A photon has three related properties: position, direction, and weight. The position of a photon is specified using three Cartesian coordinates: x, y, and z. The direction of propagation of the photon is specified using the direction cosine (u_x, u_y, u_z) to determine the photon's next position. Each photon is positioned with the same initial position of the block, denoted by x_0, y_0 and z_0. The relevant expression is:

$$x_0 = \frac{X_0}{2}, y_0 = \frac{Y_0}{2}, z_0 = 0 \quad (1)$$

For this simulation, each photon is assumed to have the same initial direction, and is perpendicular to the target surface:

$$u_{x0} = 0, u_{y0} = 0, u_{z0} = 1 \quad (2)$$

The photon moves through the clouds by taking a step in the direction currently traveling. It starts by walking along the z-axis with a random step size.

2.2 Atmospheric Transmission

Transmission is the process of propagating radiation through a cloud. It is the ratio of transmitted radiation to total radiation incident upon the cloud, measured as transmittance. Transmission in the atmosphere varies with wavelength. The scattering coefficient is wavelength dependent due to scattering across the dust and aerosol particle size distribution. The type of scattering depends on the size of the specific air particle about the transmission of wavelength.

Anisotropy, absorption, and scattering coefficients all affect transmission. This produces an attenuation of the beam power with respect to the transmitted distance, as indicated by the Beer-Lambert law. Assuming a constant atmospheric extinction coefficient, the law is as follows:

$$T_a = \exp(-\mu_{ext} Z) \quad (3)$$

Where, T_a is the one-way attenuation factor, μ_{ext} is atmospheric extinction coefficient in (mm^{-1}), and Z is range. An expression for μ_{ext}, which can be derived from the definition of visibility R_v and wavelenght λ, can be determined from experimental data, resulting in (Kruse et al., 1962):

$$\mu_{ext} = \frac{3.91}{R_v}\left(\frac{\lambda}{0.55}\right)^{-q} \quad (4)$$

Where, q is the size distribution of the scattering particles. The value of q is a function of the visibility, size, and distribution of the scattering, as determined by experimental observations and theoretical computations (Kim et al.,). Which is expressed by $q = 0.16\,R_v + 0.34$ for haze visibility (1 km $< R_v <$ 6 km), $q = R_v - 0.5$ for mist visibility (0.5 km $< R_v <$ 1 km) and $q = 0$ for fog visibility ($R_v < 0.5\ km$).

The photon moves a step in the direction to propagate through the clouds. Wilson et al. selected the step size to be random such that:

$$\Delta s = -\frac{ln\xi}{\mu_{ext}} \quad (5)$$

Where, ξ denotes a uniform random number on [0,1], and μ_{ext} is the extinction coefficient. If the weight of the photon after the collision is still greater than a threshold weight value (w_t), the photon will continue to propagate in the new direction with a distance between the two collisions equal to a photon step.

2.3 Photon Absorption

At the end of each step, some of the photon's weight is absorbed in the new position. The photon's current position is placed within the absorption matrix Q. The fraction of the photon's current weight that is lost at each step by [10]:

$$Q(i,j,k) = Q(i,j,k) + w\left(\frac{\mu_{abs}}{\mu_{ext}}\right) \quad (6)$$

Here, i, j and k represent the indices corresponding to the photon's current position. The photon's remaining weight is given by:

$$w' = \left(1 - \frac{\mu_{abs}}{\mu_{ext}}\right).w = \frac{\mu_{sca}}{\mu_{ext}}.w \quad (7)$$

2.4 Photon Scattering

The photon direction changes due to scattering off after a partial absorption event. Figure 1 shows an azimuth angle φ_{sca} in the X-Y plane and a deflection angle θ_{sca} along the Z-axis. Because scattered radiation is considered to be unpolarized, the azimuth direction is chosen to lie with equal probability on [0, 2π]. The scattering phase function φ_{sca} is expressed as

$$\varphi_{sca} = \xi.2\pi \quad (8)$$

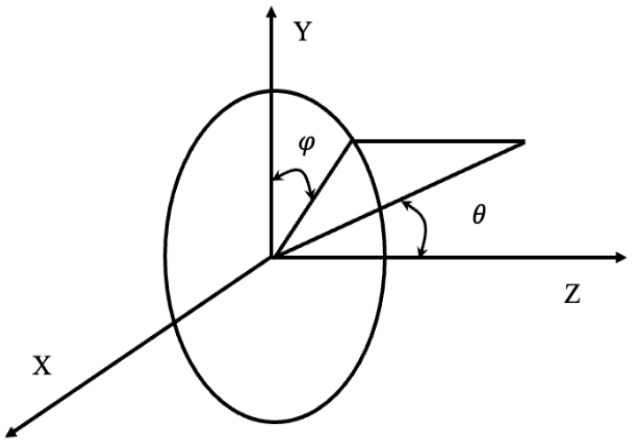

Fig. 1. Coordinate system showing azimuth and deflection angle definitions

The deflection angle θ_{SCA} defines forward (or backward). However, it is not easy to estimate a phase angle using the Mie solutions, nor to take into consideration the many sizes and shapes of particles that could be present in a single environment. The Henyey-Greenstein (HG)

function provides an approximate Mie solution (Prahl et al., 1989). The "phase problem" is roughly solved using this function in this context. To get the deflection angle, the HG phase function is adjusted (Welch and Gemert, 1995):

$$cos\theta_{SCA} = \left(\frac{\left(1+g^2-\left(\frac{1-g^2}{1-g+2g\xi}\right)^2\right)}{2g} \right) \quad (9)$$

Where g is the anisotropy factor. The anisotropy factor influences the next direction following a scattering event: forward or backward. It can vary from -1 to 1. A value g = 0 implies that scattering is completely isotropic. Transmission is higher for forward scattering ($g \rightarrow 1$) because photons are less likely to be considerably dispersed away from their original direction along the Z-axis into the clouds. As $g \rightarrow 0$, isotropic scattering increases, and the photon has a larger chance of being dispersed in any direction.

The position is determined by the angles the photon trajectory makes with each of the three Cartesian axes (u_{xx}, u_{yy}, u_{zz}). Before moving on to the next step, the trajectory of photons is updated. The direction of photon propagation is calculated by (Ilie et al., 2007):

$$\begin{cases} u_{xx} = \frac{\sin\theta_{SCA}}{\sqrt{1-u_z^2}}(u_x u_z \cos\varphi_{SCA} - u_y \sin\varphi_{SCA}) + u_x \cos\theta_{SCA} \\ u_{yy} = \frac{\sin\theta_{SCA}}{\sqrt{1-u_z^2}}(u_y u_z \cos\varphi_{SCA} + u_x \sin\varphi_{SCA}) + u_y \cos\theta_{SCA} \\ u_{zz} = -\sin\theta_{SCA}\cos\varphi_{SCA}\sqrt{1-u_z^2} + u_z \cos\theta_{SCA} \end{cases} \quad (10)$$

In the case where $u_z \cong \pm 1$ hay $|u_z| > 0.999$, the denominator of the u_{xx} and u_{yy} direction cosines becomes zero. The new direction cosines can be calculated using:

$$\begin{aligned} u_{xx} &= \sin\theta_{SCA}\cos\varphi_{SCA}, \\ u_{yy} &= \sin\theta_{SCA}\sin\varphi_{SCA}, \\ u_{zz} &= u_z/|u_z| . \cos\theta_{SCA} \end{aligned} \quad (11)$$

Where (u_x, u_y, u_z) is the direction of photon propagation before collision. Consequently, the photon moves to a new location (x', y', z'). With a step size Δs, the photon's position (x, y, z) is updated accordingly:

$$x' = x + u_{xx}.\Delta s,\ y' = y + u_{yy}.\Delta s,\ z' = z + u_{zz}.\Delta s \quad (12)$$

The photon will repeat the process of colliding with the cloud particles and scattering if its new location remains inside the cloud. The collision-propagation cycle continues until it leaves the cloud or the energy is below the threshold. Figure 2 shows the change in the propagation direction of the photon after the collision.

As the photon travels through the cloudy medium, the weight of the photon is gradually reduced with each collision event. In addition, since only a random small amount of the photon weight is removed rather than an absolute amount removed after each interaction, it is difficult to continuously track the photon weight down to zero. Therefore, the paper proposes to use an approximation. Here, the used photon weight threshold (w_t) is usually chosen as 10^{-4}. When the weight of a photon is below this threshold, it is discarded and a new photon is launched.

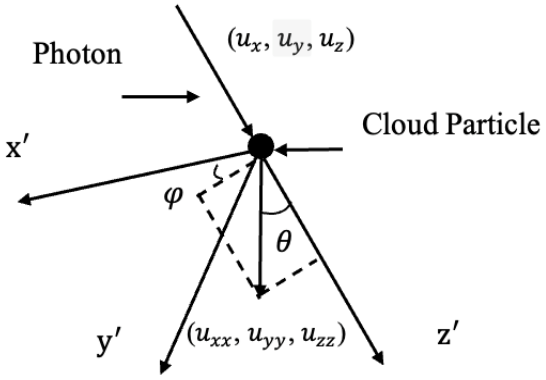

Fig. 2. Change of photon propagation direction after collision

2.5 Target Reflection

When a photon encounters a target during propagation, it is reflected by the target surface. The new direction is reversed by changing the sign of the appropriate direction angle, with no change in photon weight. Figure 3 depicts the change direction of photon propagation.

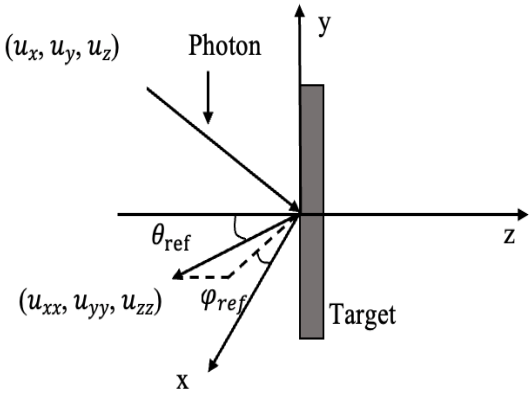

Fig. 3. Change of photon propagation direction after target reflection

3. Simulation Results and Discussion

The simulation in this paper uses the Monte-Carlo approach to generate a statistical distribution from a single point source traveling through the cloudy medium. Figure 5 shows the technique as a flowchart. At each step, the photon deposits a portion of its energy. Each step direction and duration are chosen at random, with the likelihood of a particular direction or length being defined by the simulation input parameters. Reflections at the target surface, as well as the likelihood

of their removal from the simulation, are taken into account.

The geometry of the simulation is established. The program simulates a block of light-scattering plastic in space, so here its dimensions are defined as X_0, Y_0 and Z_0, in millimeters, and the respective resolutions Δx, Δy and Δz are chosen such that.

The simulation's geometry has been established. Because the program simulates a block of light-scattering plastic in space, its dimensions are defined as X_0, Y_0 and Z_0, in millimeters, and the resolutions Δx, Δy and Δz are chosen so that

$$N_x = \frac{X_0}{\Delta x}$$
$$N_y = \frac{Y_0}{\Delta y} \quad (13)$$
$$N_z = \frac{Z_0}{\Delta z}$$

where N_x, N_y and N_z are integers representing the number of bins along each of the Cartesian direction. These numbers can vary from the tens, for low resolution cases, into the hundreds or thousands, depending on the accuracy required. These bins are used to record partial absorption by the material as photons are scattered. A matrix, labeled Q, with dimensions N_x, N_y and N_z is used to represent the block.

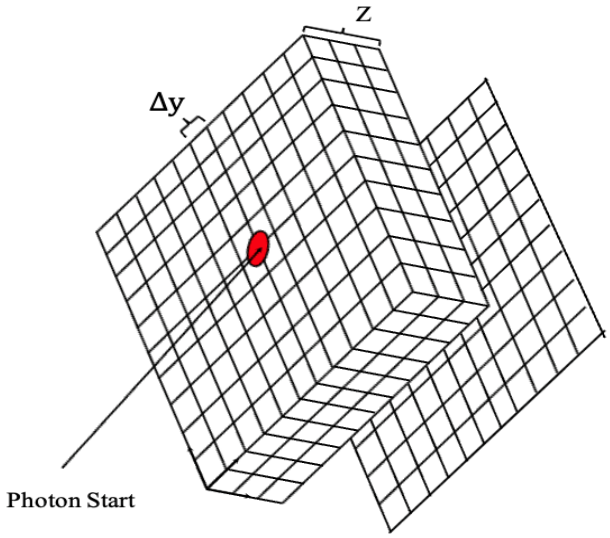

Fig. 4. Simulation block concept diagram matrix Q

With a step size chosen, the position of photon is updated accordingly to Equation (12).

As the direction of the photon has not yet been updated from the initial condition, the first step, though of variable length, is always perpendicular to the XY plane, along Z into the clouds. At every step, the position is checked to verify the photon in the cloud. For the case of a photon exceeding the target surface:

$$x_{new} = x_{current} - ux * \Delta s$$
$$y_{new} = y_{current} - uy * \Delta s \quad (14)$$
$$z_{new} = z_{current} - uz * \Delta s$$

With the photon at its previous position, the exact size of a step to the boundary along the current direction is calculated. Continuing with the case of a photon approaching the surface:

$$\Delta s_{target} = \left|\frac{z_{new}}{uz}\right| \quad (15)$$

The position is updated to bring the photon exactly to the Z surface:

$$x_{target} = x_{target} + ux * \Delta s_{target}$$
$$y_{target} = y_{target} + uy * \Delta s_{target} \quad (16)$$
$$z_{target} = z_{target} + uz * \Delta s_{target}$$

The direction of the reflected photon:

$$u_{xx} = \sin\theta_{ref}\cos\varphi_{ref}, \quad u_{yy} = \sin\theta_{ref}\sin\varphi_{ref},$$
$$u_{zz} = \cos(\pi - \theta_{ref}) \quad (17)$$

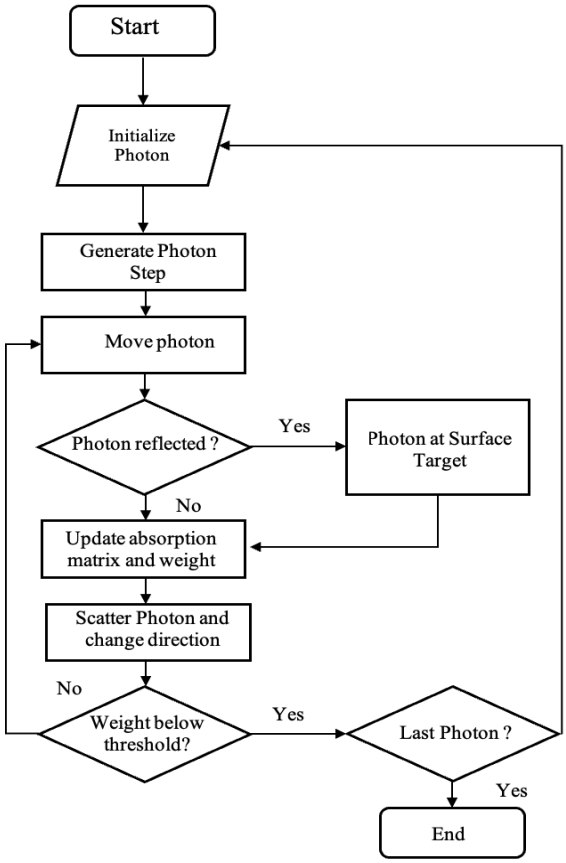

Fig. 5. Flowchart summary of the Monte Carlo Method for Photon Transport in Clouds

In this case, $z_{target} = Z_0$. There is a case of target reflection and all of the photon is returned. The direction is reversed, simply by switching the sign of the appropriate directional cosine.

$$x = x_{target} - u_{xx}.(\Delta s - \Delta s_{target})$$
$$y = y_{target} - u_{yy}.(\Delta s - \Delta s_{target}) \quad (18)$$
$$z = z_{target} - u_{zz}.(\Delta s - \Delta s_{target})$$

Furthermore, the number of photons is a significant determinant in the Monte Carlo simulation. The huge number of photons employed in a single simulation linearly increases the computing time required, but it can reduce the variance in the distribution. The energy is recorded as the number of photons received successfully by the receiver on laser fuze. The paper employs the Monte-Carlo method to generate a statistical distribution from a single point source passing through cloudy medium. The Monte Carlo method is based on two primary optical parameters: scattering coefficient and absorption coefficient.

The weight of the photon lost as its energy is deposited in a scattering event is updated to the Q matrix. Hence, the fraction of light absorbed at each step is affected. Transmission was calculated as the ratio of photons received to the total launched photons.

3.1 The Effect of Scattering and Absorption

Transmission as a function of Scattering

The scattering coefficient μ_{sca} determines the average step size of each photon. The step size, which is related to the typical lifetime of a photon inside the clouds, makes up the majority of the contribution. Higher values of μ_{sca} decrease the average step size and thus increase the number of times a photon is likely to scatter. As expected, low scattering coefficient values result in higher transmission.

Figure 6 shows transmission with absorption coefficient μ_{abs} = 0.3 mm^{-1}. It shows that higher values of μ_{sca} will decrease the average step size and thus increase the number of scattering events. Increasing the scattering coefficient from 1 mm^{-1} to 4 mm^{-1} results in a change to transmission by 30%.

Transmission as a function of Absorption

Absorption coefficient μ_{abs} affects the size of the fraction of light absorbed at each step. It makes up part of the extinction coefficient, along with μ_{sca} as well. Transmission for varying μ_{abs} is shown in Figure 7 Increasing absorption coefficient from 0.1 mm^{-1} to 0.2 mm^{-1} will reduce transmission from 95% to 90%. This implies that variable decoupling can be used during model parameter estimation. Anisotropy variables may be used initially to match a beam profile, while the absorption parameter is individually adjusted to match the corresponding experimentally estimated transmission.

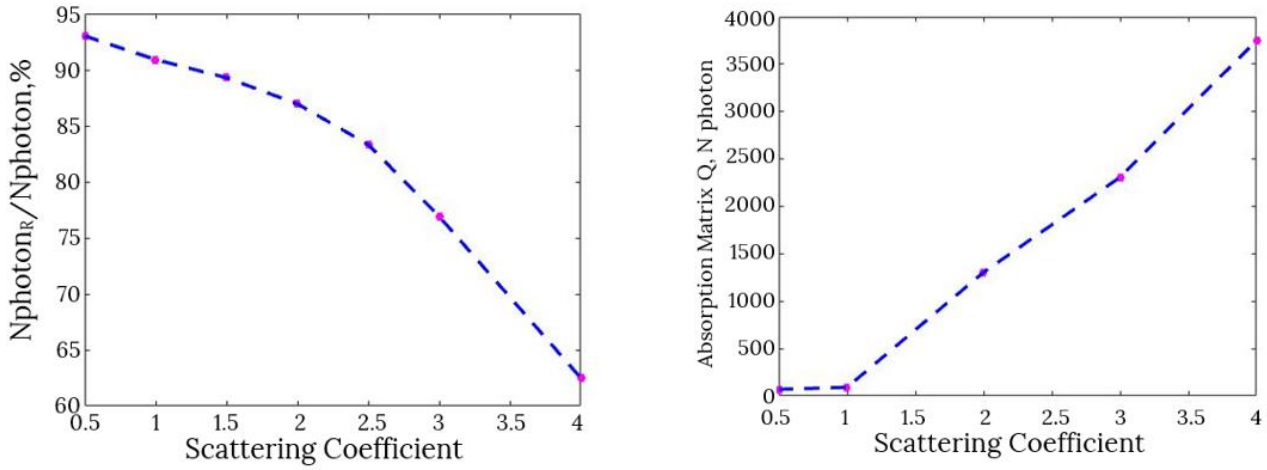

Fig. 6. Transmission as a function of Scattering coefficients

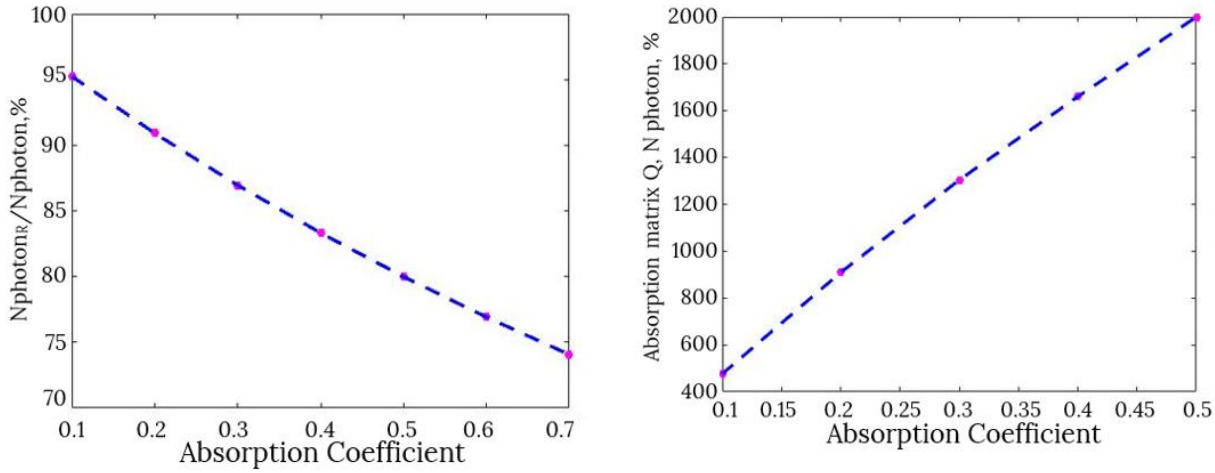

Fig. 7. Transmission as a function of Absorption coefficient

Table 1. A table of atmospheric tranmission factor as a function of visibility for 785 nm, 860 nm and 1550 nm calculated from Equation 3

Visibility (km)	785 nm		860 nm		1550 nm		Weather
	μ_{ext}	T_a	μ_{ext}	T_a	μ_{ext}	T_a	
0.05	78.200	0.2093	78.200	0.2093	78.200	0.2093	
0.2	19.550	0.6764	19.550	0.6764	19.550	0.6764	Fog
0.5	7.8200	0.8552	7.8200	0.8552	7.8200	0.8552	
0.6	6.2889	0.8818	6.2318	0.8828	5.8753	0.8891	
0.7	5.2021	0.9012	5.1080	0.9029	4.5403	0.9132	Mist
0.8	4.3927	0.9159	4.2741	0.9181	3.5817	0.9308	
0.9	3.7682	0.9274	3.6331	0.9299	2.8704	0.9442	
1	3.2728	0.9366	3.1269	0.9394	2.3291	0.9545	
2	1.5459	0.9696	1.4555	0.9713	0.9876	0.9867	Haze
4	0.6898	0.9863	0.6308	0.9875	0.3541	0.9929	
5	0.5213	0.9896	0.4698	0.9906	0.2400	0.9952	

Wavelength Dependence of Atmospheric Attenuation

The extinction coefficient μ_{ext}, which is the sum of two coefficients Absorption coefficient μ_{abs} and Scattering coefficient μ_{sca}

$$\mu_{ext} = \mu_{abs} + \mu_{sca}$$

A better understanding of laser behavior in fog, mist and haze is essential for becoming the preferred solution for selecting the appropriate wavelength to improve the detection capability of the laser fuze. As a result, the paper compares the attenuation of three different wavelengths and six different weather conditions.

The wavelength dependence of atmospheric attenuation in haze is shown in Table 1

However, empirical data for fog show that there is no wavelength dependence for atmospheric attenuation between 785 nm, 860 nm, and 1550 nm. When considering the effects of atmospheric attenuation in fog conditions with visibility less than 500 m, a laser fuze using 1550 nm has no advantage over the others.

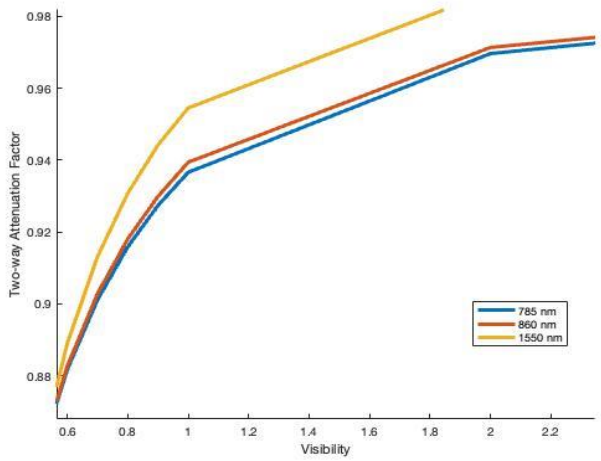

Fig. 8. Squared attenuation factor as a function of visibility

The observation, as shown in Figure 8, is that there is an inherent advantage to using 1550 nm over 780 nm and 860 nm for atmospheric attenuation in mist. If there is a slight increase in haze attenuation, the effect is minor. When there is haze, atmospheric attenuation increases as the wavelength decreases.

The echo signal is primarily composed of the reflected signal from the target, while the proportion of backscattering echo from cloud particles is very small, with a value generally not exceeding 1%. As a result, the target echo differences between laser fuze are caused primarily by differences in target reflection.

4. Conclusions

In this paper, the detection capability of proximity laser fuze in weather conditions is compared in this simulation using three distinct infrared laser wave bands by predicting the effects of laser transmission and atmospheric attenuation factor. The Monte Carlo method is used to construct a detection model that simulates laser echoes in clouds. The method simulates light propagation across various atmospheric attenuation conditions via photon transport by running thousands of photons repeatedly and adding them to a master matrix. When atmospheric attenuation is factored in, there is no advantage to using 1550 nm over 860 nm or 785 nm in fog conditions with visibility less than 500 m. There is a wavelength dependence in hazy conditions (visibility greater than 2 km), and the estimate of less atmospheric attenuation at 1550 nm is most likely correct. This study on wavelength-independent attenuation in various weather scenarios is significant because it can be used to guide and reference the use of wavelength lasers in laser fuze.

Nomenclature

HG : Henyey-Greenstein function

CRediT Author Statement

Hoang Linh Nguyen: Conceptualization, Methodology, Software, Investigation, Validation, Writing-Original Draft. **Trung Dung Pham**: Conceptualization, Methodology, Writing-Review & Editing, Visualization, Supervision. **Hong Son Tran**: Conceptualization, Methodology, Software, Investigation, Validation, Writing-Original Draft. **Thanh Chung Nguyen**: Conceptualization, Methodology, Software, Validation, Writing-Original Draft.

References

A. Welch and M. van Gemert, (1995). Optical-Thermal Response of Laser-Irradiated Tissue, *New York: Springer*.

B. Wilson and G. Adam, (1983). A Monte Carlo model for the absorption and flux distributions of light in tissue, Medical Physics, vol. 10, no. 6, pp. 824-830.

D. M. Winker and L. R. Poole, (1995). Monte-Carlo calculations of cloud returns for ground-based and space-based LIDARS, Appl. Phys. B 60, pp.341–344.

F. Q. Liu, (2017). Quantum cascade lasers: from mid-infrared to THz, *Opt. Optoelectron. Technol.*

H. X. Wang, Y. Z. Zhu, T. Tian, and A. J. Li, (2013). Characteristics of laser transmission in different types of aerosols, *Acta Phys. Sinica* 62, pp. 316– 325.

I.I.Kim,B.McArthur,and E.J.Korevaar, (2001). Comparison of laser beam propagation at 785 nm and 1550 nm in fog and haze for optical wireless communications in Optical Wireless Communications.

K. Sato, K. Yasuo, S. Takushi and S. Isao, (2002). "Laser Welding of plastics transparent to near-infrared rasdiation," in SPIE Proceedings, San Jose.

M. Ilie, J. Kneip, S. Mattei, A. Nichici, C. Roze and T. Girsole, (2007). Laser beam scattering effects in non-absorbent inhomogenous polymers, *Optics and Lasers in Engineering*, vol. 45, no. 3, pp. 405- 412.

M. Kavehrad, B. Hamzeh, (2005) “Beaming Bandwidth via Laser Communications”, 5th Integrated Communications, Navigation and Surveillance Technologies Conference (ICNS), Fairfax, Virginia.

S. Chudamani, J. D. Spinhirne, and A. D. Clarke, (1996). Lidar aerosol backscatter cross sections in the 2-μm near-infrared wavelength region, Appl. Opt. 35, pp. 4812–4819.

S. Prahl, M. Keijzer, S. Jacques and A. Welch, (1989). A Monte Carlo Model of Light Propagation in Tissue, Dosimetry of laser radiation in medicine and biology, no. 5, pp. 102-111.

T. J. Hu, Y. L. Zhao, Y. Zhao, and W. Ren, (2017). Integration design of a MEMS based fuze, *Sens. Actuat.* A 268, pp. 193–200.

V. Kagan, R. Bray and W. Kuhn, (2002) "Laser Transmission Welding of Semi-Crystalline Thermoplastics- -Part 1: Optical Characterization of Nylon Based Plastics," Journal of Reinforced Plastics and Composites, vol. 21, no. 12, pp. 1101-1122.

V. Srivastava, M. A. Jarzembski, and D. A. Bowdle, (1992). Comparison of calculated aerosol backscatter at 9.1- and 2.1-μm wavelengths, *Appl. Opt.* 31, pp. 1904–1906.

W. K. Pratt,(1969). Laser Communication Systems, *J. Wiley & Sons*, New York.

W. Kruse, L. D. McGlauchlin, and R. B. McQuistan, (1962). Elements of Infrared Technology: Generation, Transmission, and Detection, *J. Wiley & Sons, New York.*